

# Path Tracking Control of Autonomous Vehicles Subject to Deception Attacks via a Learning-Based Event-Triggered Mechanism

Zhou Gu<sup>1</sup>, Member, IEEE, Tingting Yin<sup>1</sup>, and Zhengtao Ding<sup>2</sup>, Senior Member, IEEE

**Abstract**—This article investigates the problem of event-triggered secure path tracking control of autonomous ground vehicles (AGVs) under deception attacks. To relieve the burden of the shareable vehicle communication network and to improve the tracking performance in the presence of deception attacks, a learning-based event-triggered mechanism (ETM) is proposed. Different from existing ETMs, the triggering threshold of the proposed mechanism can be dynamically adjusted with conditions of the latest vehicle state. Each vehicle in this study is deemed as an agent, under which a novel control strategy is developed for these autonomous agents with deception attacks. With the assistance of Lyapunov stability theory, sufficient conditions are obtained to guarantee the stability and stabilization of the overall system. Finally, a simulation example is provided to demonstrate the effectiveness of the proposed theoretical results.

**Index Terms**—Autonomous ground vehicles (AGVs), deception attacks, learning-based event-triggered control, path tracking.

## I. INTRODUCTION

AUTONOMOUS ground vehicles (AGVs) have gained a great popularity in society over the past decade owing to the technological innovation and security enhancement of available vehicles. The main goal of AGVs is to reduce energy consumption and travel costs, while improving road safety. Designing an appropriate control strategy for AGVs including information transmission mechanism among AGVs plays a critical role. To achieve this goal, in recent years, a remarkable number of research efforts have been dedicated to develop different control strategies for various study missions [1]–[3]. For example, Hu *et al.* [3] proposed a lane-keeping control strategy for the autonomous vehicles with prescribed performance considering the rollover prevention and input saturation. The path tracking control problem, as one of the foundational researches on AGVs, has also attracted great attention during the past years [4]. In [5], the authors focused

on the problem of robust  $H_\infty$  path following control for AGVs with time delay and data dropout. Hu *et al.* [6] developed a control strategy on path following of AGVs with limited output. In [7], a composite nonlinear feedback control rule was applied for AGV path following issue. Yu *et al.* [8] studied the cooperative path planning of target tracking for AGVs in urban environments. In [9], the problem of accelerated lane-changing trajectory planning of automated vehicles with vehicle-to-vehicle (V2V) collaboration was studied. On the basis of the existing research, it is important and challenging to further improve the contradiction between vehicles communication and control performance for networked AGV control design. To address this problem, machine learning methods were applied in AGV study, see [10]–[12], and the references therein. However, there is still much room for researches to get better results. This is our main motivation to study the learning-based event-triggered path tracking control for networked AGVs in current research.

For AGVs, information interaction is generally transmitted over a wireless network. Therefore, the network communication is essential for vehicle-coordinated control and scheduling. However, it also brings a lot of problems, such as time-delay, packet loss, and uncertainty, which may cause the system performance deterioration or even instability [13]–[16]. It consequently becomes a hot research topic on the issue of improving the network communication resources' utilization while maintaining the system performance [17]–[20]. Time-triggered mechanism (TTM) with periodic sampling period is widely utilized in the traditional networked control systems. Under such a mechanism, the data sampling and releasing are implemented at a fixed period. The worst condition should be considered before determining the fixed period. Therefore, the use of the TTM seems to be a good choice in terms of getting a satisfactory control performance and convenience of implementation. It needs to be pointed out that this mechanism may lead to the waste of communication, computation resources, and network congestion due to the release of a large amount of redundant data into the network. Numerous researchers devote themselves into developing more effective control strategy to deal with this problem [21]–[24] and the references therein. Yue *et al.* [23] first proposed the discrete ETM under which the periodic measured data were supervised at discrete instants and the sampled signal was transmitted only when the event-triggering condition was violated. Recently, a lot of achievements on the discrete ETM have been available. For example, the ETM in [23] was extended to the memory-based

Manuscript received July 29, 2020; revised October 19, 2020 and January 5, 2021; accepted January 27, 2021. Date of publication February 15, 2021; date of current version December 1, 2021. This work was supported in part by the National Natural Science Foundation of China under Grant 62022044 and Grant 61473156 and in part by the Jiangsu Natural Science Foundation for Distinguished Young Scholars under Grant BK20190039. (Corresponding author: Zhou Gu.)

Zhou Gu and Tingting Yin are with the College of Mechanical and Electronic Engineering, Nanjing Forestry University, Nanjing 210037, China (e-mail: gzh1808@163.com; yttangle@163.com).

Zhengtao Ding is with the School of Electrical and Electronic Engineering, The University of Manchester, Manchester M13 9PL, U.K. (e-mail: zhengtao.ding@manchester.ac.uk).

Color versions of one or more figures in this article are available at <https://doi.org/10.1109/TNNLS.2021.3056764>.

Digital Object Identifier 10.1109/TNNLS.2021.3056764

triggered mechanism [25], [26] and the adaptive ETM [27]. Under the adaptive ETM, the event-triggering condition is updated with the threshold variation, so as to better adapt to the requirements of control performance. For this purpose, the authors, in [27], proposed an adaptive ETM to study the problem of tracking control. Based on such a transmission mechanism, the velocity-based robust fault-tolerant automatic steering control for AGVs was investigated in [28].

AGV signal is transmitted via communication network, which is vulnerable to be attacked by malicious adversaries, especially for the shared communication network, thereby affecting the path tracking performance. In the past decades, the network security problem has become a hot topic of research. A great number of research results on cyberattacks have been available in recent years [29], [30]. Cyberattacks, discussed in the existing literature, are mainly classified into deception attacks, replay attacks, and denial-of-service (DoS) attacks. Adversaries launch deception attacks by wrecking the integrity of data packets. The DoS attack aims to block the data transmission for the purpose of compromising the availability of resources, thereby degrading the system performance. In [31], the authors studied a secure impulsive synchronization control of multi-agent systems considering the influence of deception attacks. Event-based secure leader-following consensus control for multi-agent systems subject to DoS attacks was investigated in [32]. However, few literature can be found on the issue of networked secure path tracking control of AGVs.

In this study, the issue of path tracking control is investigated for learning-based event-triggered AGVs subject to deception attacks. The contributions of this article can be summarized as follows:

- 1) A learning-based ETM is proposed to cope with limited communication and computation resources, where the triggering threshold can be adaptively adjusted according to the states of the vehicle and its adjacent vehicles via a vehicle communication network. Compared to the ETM with a prescribed constant threshold [23], the proposed learning-based ETM can dynamically adjust data releasing rate so as to get a satisfactory tracking performance when the networked AGVs are subjected to deception attacks.
- 2) A novel control strategy is developed to implement the path tracking control and ensures the stability of the AGVs with deception attacks. In the study, each vehicle of the discussed system is modeled as an agent. Different from the existing literature on AGVs [1], [4], the influence of deception attacks on the data transmission via a vehicle communication network is considered in this article, which is closer to the actual situation in practice. The feasibility of the proposed theoretical results has been verified through a simulation example.

The remainder of this article is organized as follows. Section II gives the problem formulation and AGV modeling. Main results of the learning-based event-triggered control for AGVs subject to deception attacks are presented in Section III. A simulation example is given in Section IV to demonstrate

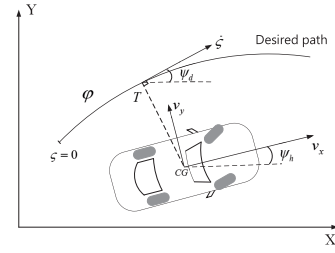


Fig. 1. Diagram of path tracking control.

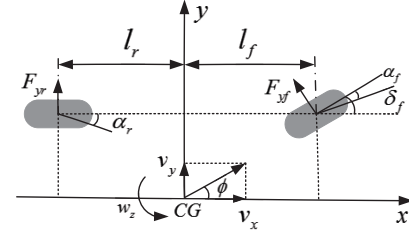


Fig. 2. Two-DoFs model of the vehicle.

the usefulness of theoretical results. Section V concludes the work of this article.

*Notation:*  $\mathbf{R}^n$  and  $\mathbf{R}^{n \times m}$  denote the  $n$ -dimensional Euclidean space and the set of  $n \times m$  real matrices, respectively;  $I$  and  $I_N$  indicate the identity matrix with appropriate dimension and the identity matrix with  $N$ -dimensional, respectively; the superscript  $T$  stands for matrix transposition;  $X > 0$  denotes that the matrix  $X$  is real symmetric positive definite.  $*$  in a symmetric matrix stands for the entries implied by symmetry.

## II. PROBLEM FORMULATION AND AGV MODELING

In this section, we first present the diagram of path tracking control of AGVs with a learning-based ETM, which is shown in Fig. 1. In what follows, the analysis and modeling for path tracking of vehicles, the learning-based ETM, deception attacks, and control strategy are presented, respectively.

### A. Modeling of Path Tracking for Vehicles

In this study, we simplify the vehicle system model to a sports bike model, which is a common approximation method for AGV motion planning. Using this method, the vehicle analysis becomes more convenient, and the control law can be designed more easily through geometric methods. As shown in Fig. 2, two degree-of-freedom (DoFs) vehicle model is utilized in this research for the controller design. The symbols in Fig. 2 are given in Table I.

For the purpose of facilitating the analysis and modeling for AGVs, we present the following assumptions.

*Assumption 1:* It is assumed that 1) the magnitude of slip angle is minor; 2) the front-wheel angle is small and tires works in the linear area; 3)  $v_x$  is a constant; 4)  $\varphi(\zeta)$  is unknown when the GPS signal is inaccessible; and 5) the heading error is small.

*Remark 1:* Based on the above assumptions, fruitful results on AGVs have been obtained, see [1], [5]–[7], and references therein. This article mainly focuses on the problem of path tracking control of networked AGVs.

TABLE I  
MEANINGS OF THE SYMBOLS IN FIGS. 1 AND 2

Symbol	Meaning
$e$	Lateral offset
$\psi_h$	Actual heading angle of the vehicle
$\psi_d$	Tangential direction of the desired path
$\psi$	Heading error, $\psi = \psi_h - \psi_d$
$w_z$	Yaw rate
$CG$	Center gravity of vehicle
$T$	Orthogonal projection point
$v_x$	Longitudinal velocities
$v_y$	Lateral velocities
$\varsigma$	Traveled distance of the point $T$ from an initial point
$\varphi(\varsigma)$	Curvature of the lane at the point $T$

From Assumption 1, the vehicle dynamics can be expressed as [6]

$$\begin{cases} v_x w_z + \dot{v}_y = \frac{1}{m}(F_{yf} + F_{yr}) \\ \dot{w}_z = \frac{1}{I_z}(l_f F_{yf} - l_r F_{yr}) \end{cases} \quad (1)$$

where  $I_z$  is the yaw inertia moment,  $m$  denotes the vehicle mass.  $l_f$  and  $l_r$  denote the length of center gravity of vehicle (CG) to the front axles and rear axles, respectively.  $F_{yf}$  and  $F_{yr}$  represent the generalized lateral tire forces of front and rear axles, respectively, which can be represented as

$$F_{yf} = C_f \alpha_f, \quad F_{yr} = C_r \alpha_r \quad (2)$$

where  $C_f$  ( $C_r$ ) is the front (rear) cornering stiffness, and the slip angle of the front (rear) wheel  $\alpha_f$  ( $\alpha_r$ ) satisfies the following equations:

$$\begin{cases} \alpha_f = \delta_f - \frac{l_f w_z}{v_x} - \phi \\ \alpha_r = \frac{l_r w_z}{v_x} - \phi \end{cases} \quad (3)$$

where  $\delta_f$  denotes the steering angle of front wheels, and  $\phi = (v_y/v_x)$ . Then, we can get  $\dot{\phi} = (\dot{v}_y/v_x)$ .

Additionally, the path tracking model shown in Fig. 1 can be presented as follows:

$$\begin{cases} \dot{e} = v_x \psi + v_y \\ \dot{\psi} = w_z - \varphi(\varsigma) v_x. \end{cases} \quad (4)$$

Combining (1)–(4), one can get the following dynamic of 2-DoFs vehicle:

$$\begin{cases} \dot{w}_z v_x = -\frac{l_f^2 C_f + l_r^2 C_r}{I_z} w_z + \frac{l_f C_f - l_r C_r}{I_z} v_y + \frac{l_f C_f v_x}{I_z} \delta_f \\ \dot{v}_y v_x = \left(-v_x^2 - \frac{l_f C_f - l_r C_r}{m}\right) w_z - \frac{C_f + C_r}{m} v_y + \frac{C_f v_x}{m} \delta_f. \end{cases} \quad (5)$$

Define  $x(t) = [w_z \phi]^T$ ,  $u(t) = \delta_f$ , then the dynamic of vehicle path tracking can be expressed as

$$\dot{x}(t) = Ax(t) + Bu(t) \quad (6)$$

where

$$A = \begin{bmatrix} a_1 & a_2 \\ a_3 & a_4 \end{bmatrix}, \quad B = \begin{bmatrix} b_1 \\ b_2 \end{bmatrix}, \quad a_1 = -\frac{l_f^2 C_f + l_r^2 C_r}{I_z v_x}$$

$$a_2 = \frac{l_r C_r - l_f C_f}{I_z}, \quad a_3 = -1 - \frac{l_f C_f - l_r C_r}{m v_x^2}$$

$$a_4 = -\frac{C_f + C_r}{m v_x}, \quad b_1 = \frac{l_f C_f}{I_z}, \quad b_2 = \frac{C_f}{m v_x}.$$

### B. Modeling of Agent-Based Vehicle Path Tracking

We define a virtual leading vehicle labeled the 0-th agent, which can be expressed as

$$\dot{x}_0(t) = Ax_0(t) + Ef(x_0(t), t) \quad (7)$$

and the other vehicles are real agents labeled as  $1, 2, \dots, N$ . The  $i$ -th vehicle is described as

$$\dot{x}_i(t) = Ax_i(t) + Bu_i(t) + Ef(x_i(t), t) \quad (8)$$

where  $f(x_i(t), t)$  is a nonlinear function.

*Remark 2:* In (7) and (8), the nonlinearity in the analysis and synthesis of path tracking control of AGVs describes inaccurate modeling and interference to the AGV.

*Remark 3:* The kinematic equation of AGVs may be more complex and diverse in real applications. In this study, each vehicle with the kinematic equation (8), shown in Fig. 3, is regarded as an agent. The further consideration for kinematics of AGVs will be discussed in the future research.

Suppose the directed topology graph of vehicle communication is  $F = (\mathcal{V}, \mathcal{E}, \mathcal{A})$ , where  $\mathcal{V} = \{1, 2, \dots, N\}$  and  $\mathcal{E} \subseteq \{(i, j), i, j \in \mathcal{V}\}$  stand for the set of nodes and edges, respectively;  $\mathcal{A} = [a_{ij}]_{N \times N}$  is a weighted adjacency matrix with nonnegative elements  $a_{ij}$  ( $i, j \in \mathcal{V}$ ). An edge  $(j, i) \in \mathcal{E}$  represents that the information of vehicle  $j$  can be received by the vehicle  $i$ .  $a_{ij} > 0$  means  $(i, j) \in \mathcal{E}$ ;  $a_{ij} = 0$  denotes  $(i, j) \notin \mathcal{E}$ . In the in-degree matrix  $D = \text{diag}\{r_1, r_2, \dots, r_N\}$ ,  $r_i = \sum_{j \in \mathbb{A}_i} a_{ij}$  for the vehicle  $i$ . The Laplacian matrix  $\mathcal{L}$  of  $F$  is defined as  $\mathcal{L} = D - \mathcal{A}$ .  $\mathbb{A}_i = \{j | (i, j) \in \mathcal{E}\}$  indicates the set of the neighbor of vehicle  $i$ .

### C. Learning-Based ETM

To economize the resources of vehicle communication network, a learning-based ETM shown in Fig. 3 is proposed. Denote the latest transmitting instant by  $t_k^i h$ , then the next transmission instant of the vehicle  $i$  is given by

$$t_{k+1}^i h = t_k^i h + \min_{g^i \geq 0} \left\{ (g^i + 1)h | \sigma_i(t) \psi_i^T(t_k^i h) \Phi_i \psi_i(t_k^i h) \right. \\ \left. < \frac{\mu}{2} [\psi_i^T(t_k^i h) \Phi_i \epsilon_i(t) + \epsilon_i^T(t) \Phi_i \psi_i(t_k^i h)] \right\} \quad (9)$$

where  $\psi_i(t_k^i h) = \sum_{j=1}^{\mathbb{A}_i} a_{ij} [x_i(t_k^i h) - x_j(t_k^i h)]$ ,  $\epsilon_i(t) = x_i(t_k^i h) - x_i(t_k^i h + g^i h)$ ,  $h$  is a sampling period, and  $\Phi_i > 0$  ( $i \in \{1, 2, \dots, N\} \triangleq \mathcal{J}$ ) is a weighting matrix. Here the sampling time sequence is denoted as  $\{kh | k \in \{0, 1, 2, \dots\} \triangleq \mathcal{N}\}$ , and the transmitting time sequence of the  $i$ th vehicle's sensor node

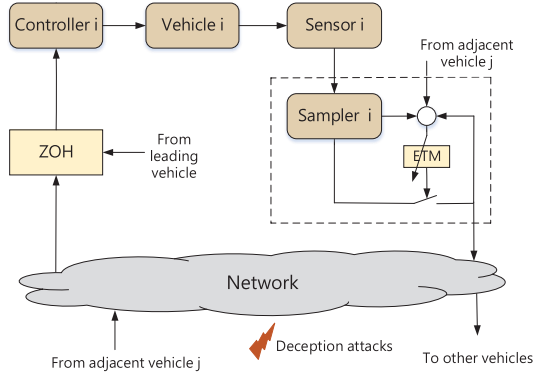


Fig. 3. Structure of the learning-based event-triggered tracking control of the vehicle  $i$  with deception attacks.

is represented as  $\{t_k^i h | t_k^i \in \mathcal{N}\}$ . The threshold  $\sigma_i(t)$  satisfies the following equality:

$$\dot{\sigma}_i(t) = \left( \frac{1}{\sigma_i^2(t)} - \frac{\sigma_a^i}{\sigma_i(t)} \right) [\psi_i^T(t_k^i h) \Phi_i \epsilon_i(t) + \epsilon_i^T(t) \Phi_i \psi_i(t_k^i h)] \quad (10)$$

where  $\sigma_a^i \geq 1$  is introduced, here, to adjust the convergence rate of  $\sigma_i(t)$ .

*Remark 4:* It is noted that the previous literatures generally used the ETM with a constant threshold such as in the literature [16], [23]. The threshold, in this study, is obtained as a result of self-learning by considering the adjacent agents' states and the self-state  $\epsilon_i(t)$ . Therefore, we call this communication mechanism as a learning-based ETM. The use of the learning-based ETM (9) can improve the resource utilization and alleviate the network bandwidth load to a large extent. In this sense, the learning-based ETM (9) plays an important role in saving network communication resources in the study of secure control for AGVs.

*Remark 5:* In this study, the learning-based ETM (9) is adopted to economize bandwidth and reduce congestion of the vehicle communication network, wherein the threshold can be dynamically adjusted according to the states of the vehicle  $i$  and its adjacent vehicles. It is worth pointing out that the learning-based control strategy has received extensive application to the analysis and design of various networked systems [34]–[36]. Motivated by the mentioned results and achievements, the learning-based ETM (9) is utilized to investigate the control problem for AGVs with deception attacks in this study.

*Remark 6:* From (10), one can see that when the system tends to be stable,  $\psi_i^T(t_k^i h) \Phi_i \epsilon_i(t) + \epsilon_i^T(t) \Phi_i \psi_i(t_k^i h) \rightarrow 0$ , in such a situation,  $\sigma_i(t)$  will tend to be a constant. If one sets  $\dot{\sigma}_i(t) \equiv 0$ , the learning-based ETM will degenerate into a conventional ETM as in [23], [32].

Considering the impact of network, we suppose  $d_{t_k}$  represents the network-induced delay of the sampling packet at instant  $t_k h$ . Then the time interval  $[t_k^i h + d_{t_k}^i, t_{k+1}^i h + d_{t_{k+1}}^i)$  can be divided into  $d_k + 1$  subintervals, namely,  $[t_k^i h + d_{t_k}^i, t_{k+1}^i h + d_{t_{k+1}}^i) = \cup_{g^i=0}^{d_k} [t_k^i h + g^i h + d_{t_k}^i, t_k^i h + g^i h + h + d_{t_{k+1}}^i)$ , where  $d_k$  is a positive constant similar to the definition in [33].

Define  $d_i(t) = t - t_k^i h - g^i h$ . One can easily know that  $0 < d_{t_k}^i \leq d_i(t) \leq h + \max\{d_{t_k}^i, d_{t_{k+1}}^i\} = h + \bar{d} \triangleq d_m$ .

Then, the state at instant  $t_k h$  of the vehicle  $i$  can be expressed by

$$\tilde{x}_i(t) = \epsilon_i(t) + x_i(t - d_i(t)) \quad (11)$$

where  $d_i(t) \in (d_n, d_m]$ ,  $d_n$  and  $d_m$  are the lower bound and upper bound of  $d(t)$ , respectively.

#### D. Deception Attacks

In AGVs, the vehicle communication network is susceptible to malicious attacks due to its openness and sharing. As depicted in Fig. 3, the deception attack is considered in this study. When the system is under deception attacks, the normal transmission data will be displaced by the attack signal  $\zeta_i(t)$ . A Bernoulli random variable  $\beta_i(t)$  is introduced to characterize the phenomenon of this kind of deception attack. Then, the real signal that the controller of vehicle  $j$  receives from vehicle  $i$  can be presented as

$$\hat{x}_i(t) = \beta_i(t) \zeta_i(t - l_i(t)) + (1 - \beta_i(t)) \tilde{x}_i(t) \quad (12)$$

under considering deception attacks, where  $\beta_i(t) \in \{0, 1\}$ ;  $\tilde{x}_i(t)$  is defined in (11) and  $\zeta_i(t)$  is defined in (13). From (12), one knows that if  $\beta_i(t) = 1$ , it implies that deception attacks occur and the transmitted signal is replaced by  $\zeta_i(t - l_i(t))$ ; if  $\beta_i(t) = 0$ , it denotes that the network does not suffer from deception attacks. In this case,  $\hat{x}_i(t) = \tilde{x}_i(t)$ . The expectation and mathematical variance of  $\beta_i(t)$  is represented as  $\bar{\beta}_i$  and  $\rho_i^2$ , respectively.  $l_i(t) \in (0, l_m)$ ,  $l_m$  is the upper bound of  $l_i(t)$ . The definition of  $l_i(t)$  is similar to  $d_i(t)$ . Here, we assume that the random variable  $\beta_i(t)$  and  $\beta_j(t)$  ( $i \neq j \in \mathcal{J}$ ) are independent.

Consider the deception attack signal  $\zeta_i(t)$  has the following format:

$$\zeta_i(t) = \check{\zeta}_i(t) - x_i(t) \quad (13)$$

where  $\check{\zeta}_i(t)$  satisfies the following sector-like bounded condition:

$$(\check{\zeta}_i(t) - H x_i(t))^T (\check{\zeta}_i(t) - H x_i(t)) \leq \theta^2 x_i^T(t) x_i(t) \quad (14)$$

where  $H$  is a known real matrix and  $\theta \geq 0$  is a known real constant.

*Remark 7:* Due to the openness and sharing of the vehicles communication network, many factors can affect the system performance of networked AGVs, including network-introduced time-delay, nonlinearity, and uncertainty, especially for cyberattacks [30]–[32]. Few literature is concerned with AGVs subject to cyberattacks. However, cyberattacks including deception attacks pose a great threat to the system performance since these attacks can block data transmission or replace transmitted signals. Therefore, this article deals with the learning-ETM-based path tracking control for networked AGVs (8) subject to deception attacks (13).

#### E. Control Strategy

Based on the above analysis, the learning-based event-triggered control strategy of the  $i$ -th vehicle is designed as

$$u_i(t) = \rho K \left\{ \sum_{j=1}^{\mathbb{A}_i} a_{ij} [\hat{x}_j(t) - \tilde{x}_i(t)] + e_i [x_0(t) - \tilde{x}_i(t)] \right\} \quad (15)$$

where  $K$  is the controller gain to be determined in Section III;  $\varrho > 0$  denotes the coupling weight of AGVs;  $a_{ij}$  stands for the adjacency element of  $F$ ; if  $e_i = 1$  means that the information of the leader can be received by the  $i$ -th vehicle.

Combining (8), (11), (12), (13), and (15), the overall AGVs can be written as

$$\begin{aligned} \dot{x}_i(t) &= Ax_i(t) + Ef(x_i(t), t) \\ &\quad - \varrho BK \left\{ \sum_{j=1}^{A_i} a_{ij} [x_i(t - d_i(t)) - x_j(t - d_j(t)) + \epsilon_i(t) \right. \\ &\quad \quad - \epsilon_j(t) - \beta_j(t)\zeta_j(t - l_j(t)) + \beta_j(t)x_j(t - l_j(t)) \\ &\quad \quad \left. + \beta_j(t)\epsilon_j(t) + \beta_j(t)x_j(t - d_j(t)) \right\} \\ &\quad \left. + e_i [x_i(t - d_i(t)) + \epsilon_i(t) - x_0(t)] \right\}. \end{aligned} \quad (16)$$

For the convenience of description, we denote

$$\begin{aligned} \eta_i(t) &= x_i(t) - x_0(t) \\ x(t) &= [x_1^T(t), x_2^T(t), \dots, x_N^T(t)]^T \\ \eta(t) &= [\eta_1^T(t), \eta_2^T(t), \dots, \eta_N^T(t)]^T \\ \epsilon(t) &= [\epsilon_1^T(t), \epsilon_2^T(t), \dots, \epsilon_N^T(t)]^T \\ \tilde{\beta}(t) &= \text{diag}\{\beta_1(t), \beta_2(t), \dots, \beta_N(t)\} \\ f(x(t), t) &= [f^T(x_1(t), t), f^T(x_2(t), t), \dots, f^T(x_N(t), t)]^T \\ \tilde{f}(x(t), t) &= [\tilde{f}_1^T(x(t), t), \tilde{f}_2^T(x(t), t), \dots, \tilde{f}_N^T(x(t), t)]^T \\ \tilde{f}_i(x(t), t) &= f(x_i(t), t) - f(x_0(t), t), \quad i = 1, 2, \dots, N \\ x(t - d(t)) &= [x_1^T(t - d_1(t)), x_2^T(t - d_2(t)), \dots, \\ &\quad x_N^T(t - d_N(t))]^T \\ x(t - l(t)) &= [x_1^T(t - l_1(t)), x_2^T(t - l_2(t)), \dots, \\ &\quad x_N^T(t - l_N(t))]^T \\ \zeta(t - l(t)) &= [\zeta_1^T(t - l_1(t)), \zeta_2^T(t - l_2(t)), \dots, \\ &\quad \zeta_N^T(t - l_N(t))]^T. \end{aligned}$$

Combining (7) and (16), one can easily obtain that

$$\begin{aligned} \dot{\eta}(t) &= (I_N \otimes A)\eta(t) + (I_N \otimes E)\tilde{f}(x(t), t) \\ &\quad - \varrho(\mathcal{L} \otimes BK)\eta(t - d(t)) - \varrho\tilde{\beta}(t)(A \otimes BK)\epsilon(t) \\ &\quad + \varrho[(A \otimes BK) - (D \otimes BK) - (D_0 \otimes BK)]\epsilon(t) \\ &\quad - \varrho\tilde{\beta}(t)(A \otimes BK)[x(t - d(t)) + x(t - l(t))] \\ &\quad + \varrho\tilde{\beta}(t)(A \otimes BK)\zeta(t - l(t)). \end{aligned} \quad (17)$$

Define  $\delta(t) = [x^T(t) \ \eta^T(t)]^T$ , the system (17) can be further written as

$$\begin{aligned} \dot{\delta}(t) &= \bar{A}\delta(t) + \bar{E}F(x(t), t) + \varrho B_1 K_2 \delta(t - d(t)) \\ &\quad + \varrho B_2 K_1 \epsilon(t) + \varrho \beta(t) B_3 K_2 [\delta(t - d(t)) + \delta(t - l(t))] \\ &\quad - \varrho \beta(t) B_4 K_1 \epsilon(t) + \varrho \beta(t) B_4 K_1 \zeta(t - l(t)) \end{aligned} \quad (18)$$

where

$$\begin{aligned} F(x(t), t) &= \begin{bmatrix} f(x(t), t) \\ \tilde{f}(x(t), t) \end{bmatrix}, \quad \beta(t) = \text{diag}\{\tilde{\beta}(t), \tilde{\beta}(t)\} \\ \bar{A} &= \text{diag}\{I_N \otimes A, I_N \otimes A\} \\ \bar{E} &= \text{diag}\{I_N \otimes E, I_N \otimes E\} \\ L &= \mathcal{L} + E_0, \quad E_0 = \text{diag}\{e_1, e_2, \dots, e_N\} \end{aligned}$$

$$K_1 = I_N \otimes K, \quad K_2 = I_{2N} \otimes K$$

$$B_1 = \begin{bmatrix} 0 & -(L \otimes B) \\ 0 & -(L \otimes B) \end{bmatrix}$$

$$B_2 = \begin{bmatrix} (A \otimes B) - (D \otimes B) - (E_0 \otimes B) \\ (A \otimes B) - (D \otimes B) - (E_0 \otimes B) \end{bmatrix}$$

$$B_3 = \begin{bmatrix} -(A \otimes B) & 0 \\ -(A \otimes B) & 0 \end{bmatrix}, \quad B_4 = \begin{bmatrix} A \otimes B \\ A \otimes B \end{bmatrix}.$$

The main purpose of this article is to develop a novel control strategy for path tracking of AGVs with deception attacks under the proposed learning-based ETM (9) to alleviate the load of the network bandwidth.

### III. MAIN RESULTS

In this section, we will present the main results of this article in the form of two theorems. The following assumption is introduced to help us obtain the main results.

*Assumption 2* [16], [21]: For the nonlinear function  $f: \mathbb{R}^2 \rightarrow \mathbb{R}^2$ , the Lipschitz condition is satisfied, which means that there exists a scalar  $\nu > 0$  such that the following inequality holds for all  $x, y \in \mathbb{R}^2$

$$\|f(x) - f(y)\| \leq \nu \|x - y\|. \quad (19)$$

*Theorem 1:* For known scalar  $\tilde{\beta}_i \in (0, 1)$ , positive scalars  $\sigma_a^i, \mu, \nu, d_n, d_m, l_m, \varrho, e_j$ , and matrix  $K$ , the system (18) is asymptotically stable in the mean-square sense, if there exist positive definite matrices  $Q_j, R_j, P, \Phi_i$  ( $i \in \mathcal{J}, j = 1, 2, 3$ ), and matrices  $N_2, N_3$  with appropriate dimensions such that the following inequalities hold:

$$\begin{aligned} \Theta &= \begin{bmatrix} \Psi_{11} & * & * & * & * \\ \Psi_{21} & \Psi_{22} & * & * & * \\ \Psi_{31} & \Psi_{32} & \Psi_{33} & * & * \\ \Psi_{41} & \Psi_{42} & \Psi_{43} & \Psi_{44} & * \\ \Psi_{51} & \Psi_{52} & \Psi_{53} & 0 & \Psi_{55} \end{bmatrix} < 0 \quad (20) \\ &\quad \begin{bmatrix} R_2 & * \\ N_2 & R_2 \end{bmatrix} > 0, \quad \begin{bmatrix} R_3 & * \\ N_3 & R_3 \end{bmatrix} > 0 \quad (21) \end{aligned}$$

where

$$\begin{aligned} \Psi_{11} &= \begin{bmatrix} \Pi_1 & * & * \\ R_1 & -Q_1 - R_1 - R_2 & * \\ \Pi_2 & R_2 + N_2 & \Pi_3 \end{bmatrix} \\ \Pi_1 &= (I_{2N} \otimes P)\bar{A} + \bar{A}^T(I_{2N} \otimes P) + Q_1 + Q_2 + Q_3 \\ &\quad - R_1 - R_3, \quad H_1 = [I_{2N} \ 0], \quad H_2 = [0 \ I_{2N}] \\ \Pi_2 &= \varrho K_2^T B_2^T (I_{2N} \otimes P) + \varrho K_2^T B_3^T (I_{2N} \otimes P) \\ \Pi_3 &= -2R_2 - N_2 - N_2^T + \frac{2}{\mu} H_1^T \mathcal{L}^T \Phi \mathcal{L} H_1 \\ \Psi_{21} &= \begin{bmatrix} 0 & -N_2 & R_2 + N_2 \\ \Pi_4 & 0 & 0 \\ -N_3 & 0 & 0 \end{bmatrix} \\ \Pi_4 &= \varrho K_2^T B_3^T \tilde{\beta}(I_{2N} \otimes P) + R_3 + N_3 \\ \Psi_{22} &= \begin{bmatrix} -Q_2 - R_2 & * & * \\ 0 & \Pi_5 & * \\ 0 & R_3 + N_3 & -Q_3 - R_3 \end{bmatrix} \\ \Pi_5 &= -2R_3 - N_3 - N_3^T + \theta^2 H_1^T (I_N \otimes P) H_1 \\ &\quad + H_1^T (I_N \otimes H^T P H) H_1 \end{aligned}$$

$$\Psi_{31} = \begin{bmatrix} H_2 \bar{E}^T (I_{2N} \otimes P) & 0 & 0 \\ \Pi_6 & -\sigma_a \Phi \mathcal{L} H_1 & 0 \\ \varrho K_1^T B_4^T \bar{\beta} (I_{2N} \otimes P) & 0 & 0 \\ \nu H_2 & 0 & 0 \end{bmatrix} \quad \begin{bmatrix} \bar{R}_2 & * \\ \bar{N}_2 & \bar{R}_2 \end{bmatrix} > 0, \quad \begin{bmatrix} \bar{R}_3 & * \\ \bar{N}_3 & \bar{R}_3 \end{bmatrix} > 0 \quad (23)$$

where

$$\Pi_6 = \varrho K_1^T B_2^T (I_{2N} \otimes P) - \varrho K_1^T B_4^T \bar{\beta} (I_{2N} \otimes P)$$

$$\sigma_a = \text{diag}\{I_2 \otimes \sigma_a^1, I_2 \otimes \sigma_a^2, \dots, I_2 \otimes \sigma_a^N\}$$

$$\Psi_{32} = \begin{bmatrix} 0 & 0 & 0 \\ 0 & 0 & 0 \\ 0 & (I_N \otimes P H) H_1 & 0 \\ 0 & 0 & 0 \end{bmatrix}$$

$$\Psi_{33} = \text{diag}\{-I, -I, -(I_N \otimes P), -I\}$$

$$\Psi_{41} = \begin{bmatrix} d_n (I_{2N} \otimes P) \bar{A} & 0 & d_n \varrho P_{12} + d_n \varrho \bar{\beta} P_{32} \\ d_1 (I_{2N} \otimes P) \bar{A} & 0 & d_1 \varrho P_{12} + d_1 \varrho \bar{\beta} P_{32} \\ l_m (I_{2N} \otimes P) \bar{A} & 0 & l_m \varrho P_{12} + l_m \varrho \bar{\beta} P_{32} \end{bmatrix}$$

$$P_{12} = (I_{2N} \otimes P) B_1 K_2, \quad P_{32} = (I_{2N} \otimes P) B_3 K_2$$

$$\Psi_{42} = \begin{bmatrix} 0 & d_n \varrho \bar{\beta} P_{32} & 0 \\ 0 & d_1 \varrho \bar{\beta} P_{32} & 0 \\ 0 & l_m \varrho \bar{\beta} P_{32} & 0 \end{bmatrix}, \quad d_1 = d_m - d_n$$

$$\Psi_{43} = \begin{bmatrix} d_n P_E & d_n \varrho P_{21} - d_n \varrho \bar{\beta} P_{41} & d_n \varrho \bar{\beta} P_{41} \\ d_1 P_E & d_1 \varrho P_{21} - d_1 \varrho \bar{\beta} P_{41} & d_1 \varrho \bar{\beta} P_{41} \\ l_m P_E & l_m \varrho P_{21} - l_m \varrho \bar{\beta} P_{41} & l_m \varrho \bar{\beta} P_{41} \end{bmatrix}$$

$$P_{21} = (I_{2N} \otimes P) B_2 K_1, \quad P_{41} = (I_{2N} \otimes P) B_4 K_1$$

$$P_E = (I_{2N} \otimes P) \bar{E} H_2^T, \quad \Phi = \text{diag}\{\Phi_1, \Phi_2, \dots, \Phi_N\}$$

$$\Psi_{51} = \begin{bmatrix} 0 & 0 & d_n \varrho \rho P_{32} \\ 0 & 0 & d_1 \varrho \rho P_{32} \\ 0 & 0 & l_m \varrho \rho P_{32} \end{bmatrix}, \quad \Psi_{52} = \begin{bmatrix} 0 & d_n \varrho \rho P_{32} & 0 \\ 0 & d_1 \varrho \rho P_{32} & 0 \\ 0 & l_m \varrho \rho P_{32} & 0 \end{bmatrix}$$

$$\Psi_{53} = \begin{bmatrix} 0 & -d_n \varrho \rho P_{41} & d_n \varrho \rho P_{41} \\ 0 & -d_1 \varrho \rho P_{41} & d_1 \varrho \rho P_{41} \\ 0 & -l_m \varrho \rho P_{41} & l_m \varrho \rho P_{41} \end{bmatrix}$$

$$\Psi_{44} = \text{diag}\{-(I_{2N} \otimes P) R_1^{-1} (I_{2N} \otimes P), \\ -(I_{2N} \otimes P) R_2^{-1} (I_{2N} \otimes P), \\ -(I_{2N} \otimes P) R_3^{-1} (I_{2N} \otimes P)\}$$

$$\Psi_{55} = \Psi_{44}, \quad \bar{\beta} = \text{diag}\{\bar{\beta}_1, \bar{\beta}_2\}$$

$$\bar{\beta} = \text{diag}\{\bar{\beta}_1, \dots, \bar{\beta}_N\}, \quad \rho_i = \sqrt{\bar{\beta}_i(1 - \bar{\beta}_i)}$$

$$\rho = \text{diag}\{\bar{\rho}_1, \bar{\rho}_2\}, \quad \bar{\rho} = \text{diag}\{\rho_1, \dots, \rho_N\}.$$

*Proof:* See Appendix A.

Sufficient conditions are obtained in Theorem 1 to ensure the asymptotic mean-square stability of the system (18). In the following, the controller gain of the learning-based event-triggered AGVs with deception attacks will be derived in Theorem 2 based on the result of Theorem 1.

*Theorem 2:* For given scalar  $\bar{\beta}_i \in (0, 1)$ , positive scalars  $\sigma_a^i, \mu, \nu, d_n, d_m, l_m, \varrho, e_j$ , the system (18) is asymptotically stable in the mean-square sense, if there exist positive definite matrices  $\bar{Q}_j, \bar{R}_j, X, \bar{\Phi}_i$  ( $i \in \mathcal{I}, j = 1, 2, 3$ ) and matrices  $Y, \bar{N}_2, \bar{N}_3$  with appropriate dimensions such that the following linear matrix inequalities hold:

$$\bar{\Theta} = \begin{bmatrix} \bar{\Psi}_{11} & * & * & * & * \\ \bar{\Psi}_{21} & \bar{\Psi}_{22} & * & * & * \\ \bar{\Psi}_{31} & \bar{\Psi}_{32} & \bar{\Psi}_{33} & * & * \\ \bar{\Psi}_{41} & \bar{\Psi}_{42} & \bar{\Psi}_{43} & \bar{\Psi}_{44} & * \\ \bar{\Psi}_{51} & \bar{\Psi}_{52} & \bar{\Psi}_{53} & 0 & \bar{\Psi}_{55} \end{bmatrix} < 0 \quad (22)$$

$$\bar{\Psi}_{11} = \begin{bmatrix} \bar{\Pi}_1 & * & * \\ \bar{R}_1 & -\bar{Q}_1 - \bar{R}_1 - \bar{R}_2 & * \\ \varrho Y_2^T B_2^T + \varrho Y_2^T B_3^T \bar{\beta} & \bar{R}_2 + \bar{N}_2 & \bar{\Pi}_2 \end{bmatrix}$$

$$\bar{\Pi}_1 = \bar{A} X_2 + X_2 \bar{A}^T + \bar{Q}_1 + \bar{Q}_2 + \bar{Q}_3 - \bar{R}_1 - \bar{R}_3$$

$$\bar{\Pi}_2 = -2\bar{R}_2 - \bar{N}_2 - \bar{N}_2^T + \frac{2}{\mu} H_1^T \mathcal{L}^T \Phi \mathcal{L} H_1$$

$$\bar{\Psi}_{21} = \begin{bmatrix} 0 & -\bar{N}_2 & \bar{R}_2 + \bar{N}_2 \\ \varrho Y_2^T B_3^T \bar{\beta} + \bar{R}_3 + \bar{N}_3 & 0 & 0 \\ -\bar{N}_3 & 0 & 0 \end{bmatrix}$$

$$\bar{\Psi}_{22} = \begin{bmatrix} -\bar{Q}_2 - \bar{R}_2 & * & * \\ 0 & \bar{\Pi}_3 & * \\ 0 & \bar{R}_3 + \bar{N}_3 & -\bar{Q}_3 - \bar{R}_3 \end{bmatrix}$$

$$\bar{\Pi}_3 = -2\bar{R}_3 - \bar{N}_3 - \bar{N}_3^T + \theta^2 H_1^T X_1 H_1 \\ + H_1^T (I_N \otimes H^T) X_1 (I_N \otimes H) H_1$$

$$\bar{\Psi}_{31} = \begin{bmatrix} H_2 \bar{E}^T & 0 & 0 \\ \varrho Y_1^T B_2^T - \varrho Y_1^T B_4^T \bar{\beta} & -\sigma_a \bar{\Phi} \mathcal{L} H_1 & 0 \\ \varrho Y_1^T B_4^T \bar{\beta} & 0 & 0 \\ \nu H_2 X_2 & 0 & 0 \end{bmatrix}$$

$$\bar{\Psi}_{32} = \begin{bmatrix} 0 & 0 & 0 \\ 0 & 0 & 0 \\ 0 & (I_N \otimes H) H_1 X_2 & 0 \\ 0 & 0 & 0 \end{bmatrix}$$

$$\bar{\Psi}_{33} = \text{diag}\{-I, -I, -X_1, -I\}$$

$$\bar{\Phi} = \text{diag}\{\bar{\Phi}_1, \bar{\Phi}_2, \dots, \bar{\Phi}_N\}$$

$$\sigma_a = \text{diag}\{I_2 \otimes \sigma_a^1, I_2 \otimes \sigma_a^2, \dots, I_2 \otimes \sigma_a^N\}$$

$$\bar{\Psi}_{41} = \begin{bmatrix} d_n \bar{A} X_2 & 0 & d_n \varrho B_1 Y_2 + d_n \varrho \bar{\beta} B_3 Y_2 \\ d_1 \bar{A} X_2 & 0 & d_1 \varrho B_1 Y_2 + d_1 \varrho \bar{\beta} B_3 Y_2 \\ l_m \bar{A} X_2 & 0 & l_m \varrho B_1 Y_2 + l_m \varrho \bar{\beta} B_3 Y_2 \end{bmatrix}$$

$$\bar{\Psi}_{42} = \begin{bmatrix} 0 & d_n \varrho \bar{\beta} B_3 Y_2 & 0 \\ 0 & d_1 \varrho \bar{\beta} B_3 Y_2 & 0 \\ 0 & l_m \varrho \bar{\beta} B_3 Y_2 & 0 \end{bmatrix}, \quad d_1 = d_m - d_n$$

$$\bar{\Psi}_{43} = \begin{bmatrix} d_n \bar{E} H_2^T & d_n \varrho B_2 Y_1 - d_n \varrho \bar{\beta} B_4 Y_1 & d_n \varrho \bar{\beta} B_4 Y_1 \\ d_1 \bar{E} H_2^T & d_1 \varrho B_2 Y_1 - d_1 \varrho \bar{\beta} B_4 Y_1 & d_1 \varrho \bar{\beta} B_4 Y_1 \\ l_m \bar{E} H_2^T & l_m \varrho B_2 Y_1 - l_m \varrho \bar{\beta} B_4 Y_1 & l_m \varrho \bar{\beta} B_4 Y_1 \end{bmatrix}$$

$$\bar{\Psi}_{51} = \begin{bmatrix} 0 & 0 & d_n \varrho \rho B_3 Y_2 \\ 0 & 0 & d_1 \varrho \rho B_3 Y_2 \\ 0 & 0 & l_m \varrho \rho B_3 Y_2 \end{bmatrix}, \quad \bar{\Psi}_{52} = \begin{bmatrix} 0 & d_n \varrho \rho B_3 Y_2 & 0 \\ 0 & d_1 \varrho \rho B_3 Y_2 & 0 \\ 0 & l_m \varrho \rho B_3 Y_2 & 0 \end{bmatrix}$$

$$\bar{\Psi}_{53} = \begin{bmatrix} 0 & -d_n \varrho \rho B_4 Y_1 & d_n \varrho \rho B_4 Y_1 \\ 0 & -d_1 \varrho \rho B_4 Y_1 & d_1 \varrho \rho B_4 Y_1 \\ 0 & -l_m \varrho \rho B_4 Y_1 & l_m \varrho \rho B_4 Y_1 \end{bmatrix}$$

$$\bar{\Psi}_{44} = \text{diag}\{-2\gamma_1 X_2 + \gamma_1^2 \bar{R}_1, -2\gamma_2 X_2 + \gamma_2^2 \bar{R}_2, \\ 2\gamma_3 X_2 + \gamma_3^2 \bar{R}_3\}$$

$$\bar{\Psi}_{55} = \bar{\Psi}_{44}, \quad H_1 = [I_{2N} \ 0], \quad H_2 = [0 \ I_{2N}]$$

$$Y_1 = I_N \otimes Y, \quad Y_2 = I_{2N} \otimes Y$$

$$X_1 = I_N \otimes X, \quad X_2 = I_{2N} \otimes X$$

$$\bar{\beta} = \text{diag}\{\bar{\beta}_1, \bar{\beta}_2\}, \quad \bar{\beta} = \text{diag}\{\bar{\beta}_1, \dots, \bar{\beta}_N\}, \quad \rho_i = \sqrt{\bar{\beta}_i(1 - \bar{\beta}_i)}$$

$$\rho = \text{diag}\{\bar{\rho}_1, \bar{\rho}_2\}, \quad \bar{\rho} = \text{diag}\{\rho_1, \dots, \rho_N\}.$$

TABLE II  
VEHICLE PARAMETERS

Physical quantity	Values
$l_f$ (m)	1.18
$l_r$ (m)	1.77
$C_f$ (N/rad)	80000
$C_r$ (N/rad)	80000
$v_x$ (m/s)	30
$m$ (kg)	1832
$I_z$ (kg·m <sup>2</sup> )	2488

Furthermore, the controller gain of the learning-based event-triggered AGVs is designed as

$$K = YX^{-1}. \quad (24)$$

*Proof:* According to  $(R_\kappa - \gamma_\kappa^{-1}(I_{2N} \otimes P))R_\kappa^{-1}(R_\kappa - \gamma_\kappa^{-1}(I_{2N} \otimes P)) \geq 0$ , it yields that

$$-(I_{2N} \otimes P)R_\kappa^{-1}(I_{2N} \otimes P) \leq -2\gamma_\kappa(I_{2N} \otimes P) + \gamma_\kappa^2 R_\kappa$$

for  $\kappa = 1, 2, 3$ , from which one can know that a new inequality is hold by replacing the terms  $-(I_{2N} \otimes P)R_\kappa^{-1}(I_{2N} \otimes P)$  ( $\kappa = 1, 2, 3$ ) in  $\Psi_{44}$  and  $\Psi_{55}$  in Theorem 1 with  $-2\gamma_\kappa(I_{2N} \otimes P) + \gamma_\kappa^2 R_\kappa$  ( $\kappa = 1, 2, 3$ ), respectively.

Let  $X = P^{-1}$ ,  $X_1 = I_N \otimes X$ ,  $X_2 = I_{2N} \otimes X$ ,  $\Sigma_1 = \text{diag}\{X_2, X_2, X_2, X_2, X_2, X_2, I, X_1, X_1, I, X_2, X_2, X_2, X_2, X_2, X_2, \}$ . Then pre- and post-multiply  $\Theta$  in (20) with  $\Sigma_1$  and  $\Sigma_1^T$ . By defining  $Y = KX$ ,  $Y_2 = I_{2N} \otimes Y$ ,  $Y_1 = I_N \otimes Y$ ,  $\tilde{\Phi} = X_1\Phi X_1$ ,  $\tilde{Q}_1 = X_2Q_1X_2$ ,  $\tilde{Q}_2 = X_2Q_2X_2$ ,  $\tilde{Q}_3 = X_2Q_3X_2$ ,  $\tilde{R}_1 = X_2R_1X_2$ ,  $\tilde{R}_2 = X_2R_2X_2$ ,  $\tilde{R}_3 = X_2R_3X_2$ ,  $\tilde{N}_2 = X_2N_2X_2$ ,  $\tilde{N}_3 = X_2N_3X_2$ , we can get  $\tilde{\Theta} < 0$  holds. Similarly, for inequalities in (21), pre- and post-multiplying them with  $\Sigma_2$  and  $\Sigma_2^T$  ( $\Sigma_2 = \text{diag}\{X_2, X_2\}$ ), respectively, one can know that the inequalities in (23) hold. On account of the results in Theorem 1, the conclusion comes that if (20) and (21) hold, the system (18) is asymptotically stable in the mean square sense. The controller gain  $K = YX^{-1}$  follows from  $Y = KX$ . That completes the proof. ■

#### IV. SIMULATION EXAMPLES

In this section, we will present a simulation example to demonstrate the effectiveness of our proposed theoretical results. Consider AGVs consisting of three vehicles, and the vehicle parameters utilized in the simulation are given in Table II.

The 0-th agent in Fig. 4 is the virtual leader of the AGVs and the communication topology graph of AGVs is shown in Fig. 4, from which one can get the Laplacian matrix as follows:

$$\mathcal{L} = \begin{bmatrix} 1 & -1 & 0 \\ 0 & 1 & -1 \\ -1 & -1 & 2 \end{bmatrix}.$$

The initial conditions are chosen by  $x_0 = [0.4 \ 0.5]^T$ ,  $x_1 = [0.5 \ 0.4]^T$ ,  $x_2 = [0.3 \ 0.2]^T$ ,  $x_3 = [0.2 \ 0.1]^T$  and  $\sigma_1(0) = 1.6$ ,  $\sigma_2(0) = 0.8$ ,  $\sigma_3(0) = 0.9$ .

The signals among AGVs are transmitted via the communication network. Assume the lower and upper bound of

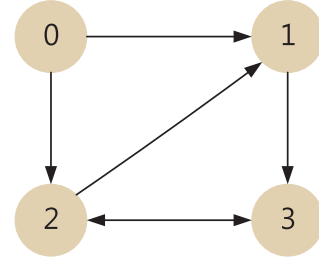


Fig. 4. Communication topology graph of AGVs.

the network-induced time delay is  $d_n = 0.01$ ,  $d_m = 0.3$ ,  $l_m = 0.15$ .

In the following, two cases are provided for demonstrating the effectiveness of the designed method, which are based on the presence or absence of deception attacks.

*Case 1:* There is no deception attacks on the vehicle communication networks.

In this situation, we set  $\bar{\beta}_1 = 0$ ,  $\bar{\beta}_2 = 0$ ,  $\bar{\beta}_3 = 0$ . Let  $\nu = 0.2$ ,  $\sigma_a^1 = 1$ ,  $\sigma_a^2 = 2$ ,  $\sigma_a^3 = 3$ ,  $\mu = 1$ ,  $\rho = 0.1$ ,  $h = 0.1$  s and  $\gamma_1 = \gamma_2 = \gamma_3 = 0.5$ . By solving linear matrix inequalities in Theorem 2, the following parameters can be easily obtained:

$$Y = [0.0037 \ 0.0427], \quad X = \begin{bmatrix} 40.3701 & 2.1328 \\ 2.1328 & 3.8802 \end{bmatrix}$$

$$K = [-0.0005 \ 0.0113], \quad \Phi_1 = \begin{bmatrix} -0.6031 & 0.0853 \\ 0.0853 & -0.1400 \end{bmatrix}$$

$$\Phi_2 = \begin{bmatrix} -0.0656 & -0.0099 \\ -0.0099 & -0.7359 \end{bmatrix}, \quad \Phi_3 = \begin{bmatrix} -0.1633 & 0.0065 \\ 0.0065 & -0.0906 \end{bmatrix}.$$

Fig. 5 shows simulation results under Case 1. The state response  $x_i(t)$ , state error  $\eta_i(t)$ ,  $i = 1, 2, 3$ , and the controller input  $u_i(t)$  of each vehicle are exhibited, from which one can see that the designed control strategy can lead to a good control performance of AGVs when there is no deception attack on the vehicle communication network.

*Case 2:* There are intermittent deception attacks on the vehicle communication network.

Under this scenario, we assume that  $\bar{\beta}_1 = 0.3$ ,  $\bar{\beta}_2 = 0.25$ ,  $\bar{\beta}_3 = 0.4$ , and the attacks satisfy inequality (14) with  $H = \text{diag}\{0.25, 0.15\}$  for  $\theta = 0$ . Let  $\nu = 0.2$ ,  $\sigma_a^1 = 1$ ,  $\sigma_a^2 = 2$ ,  $\sigma_a^3 = 3$ ,  $\mu = 1$ ,  $\rho = 0.1$ ,  $h = 0.1$  s and  $\gamma_1 = \gamma_2 = \gamma_3 = 0.5$ . By solving linear matrix inequalities in Theorem 2, one can obtain that

$$Y = [0.0035 \ 0.0472], \quad X = \begin{bmatrix} 40.3470 & 2.1288 \\ 2.1288 & 3.8811 \end{bmatrix}$$

$$K = [-0.0006 \ 0.0125], \quad \Phi_1 = \begin{bmatrix} -0.6030 & 0.0852 \\ 0.0852 & -0.1463 \end{bmatrix}$$

$$\Phi_2 = \begin{bmatrix} -0.0651 & -0.0093 \\ -0.0093 & -0.7523 \end{bmatrix}, \quad \Phi_3 = \begin{bmatrix} -0.1656 & 0.0052 \\ 0.0052 & -0.0929 \end{bmatrix}.$$

Figs. 6–9 present path tracking results of networked AGVs under Case 2. Fig. 6 depicts the state response  $x_i(t)$ , the path tracking error  $\eta_i(t)$ , and the controller input  $u_i(t)$  of each vehicles for  $i = 1, 2, 3$ , respectively. The distribution of deception attacks that satisfy (14) is shown in Fig. 7. From Fig. 6, it can be concluded that the path tracking of AGVs under this intermittent deception attacks can also perform well. Fig. 8 gives the threshold of each learning-based ETM  $\sigma_i(t)$

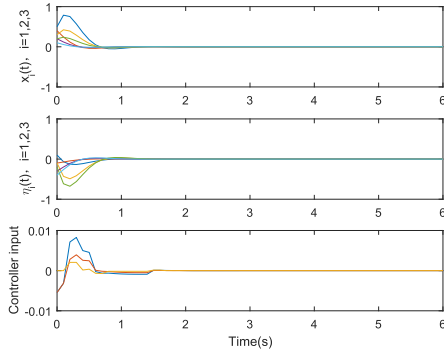


Fig. 5. State response  $x_i(t)$ , state error  $\eta_i(t)$ , and controller input  $u_i(t)$  ( $i = 1, 2, 3$ ) under Case 1.

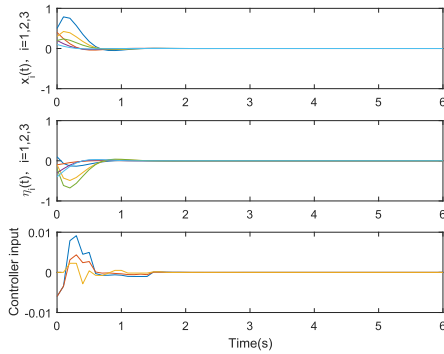


Fig. 6. State response  $x_i(t)$ , state error  $\eta_i(t)$ , and controller input  $u_i(t)$  ( $i = 1, 2, 3$ ) under Case 2.

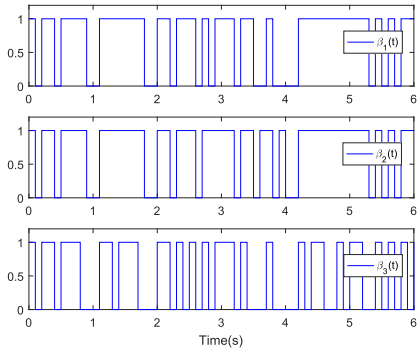


Fig. 7. The distribution of  $\beta_1(t)$  with  $\bar{\beta}_1 = 0.3$ ,  $\beta_2(t)$  with  $\bar{\beta}_2 = 0.25$ , and  $\beta_3(t)$  with  $\bar{\beta}_3 = 0.4$  under Case 2.

( $i = 1, 2, 3$ ). Fig. 9 exhibits the release time intervals of three vehicles with the proposed learning-based ETM, respectively, from which one can see that a large amount of sampling data is dropped out before releasing into the network, thereby relieving the burden of limited network bandwidth.

*Remark 8:* From Fig. 8, one can see that the learning-based triggering threshold  $\sigma_i(t)$  ( $i = 1, 2, 3$ ) is a self-learning procedure, and finally converges to a constant when the system is stable. Compared to the literature [23] with a consist threshold, the threshold  $\sigma_i(t)$  in this study can dynamically adjusted based on the releasing instant, vehicle state, along with itself state. In this example, if one gives the initial parameters  $\sigma_1(0) = 1.6$ ,  $\sigma_2(0) = 0.8$ ,  $\sigma_3(0) = 0.9$  and  $\sigma_a^1 = 1$ ,  $\sigma_a^2 = 2$ ,  $\sigma_a^3 = 3$ , then  $\sigma_1(t)$ ,  $\sigma_2(t)$ , and  $\sigma_3(t)$  converge to 1.627, 0.807, and 0.9102, respectively. In this case of  $\sigma_1(t) = 1.627$ ,  $\sigma_2(t) = 0.807$ , and  $\sigma_3(t) = 0.9102$ , it turns to be a conventional event-triggered scheme.

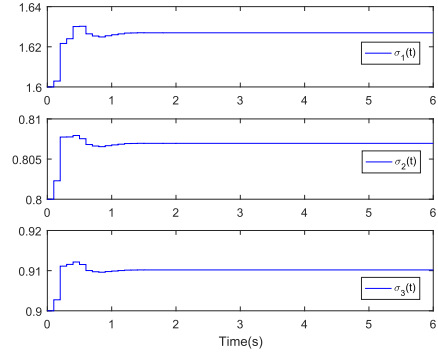


Fig. 8. Threshold of each learning-based ETM  $\sigma_i(t)$  ( $i = 1, 2, 3$ ) under Case 2.

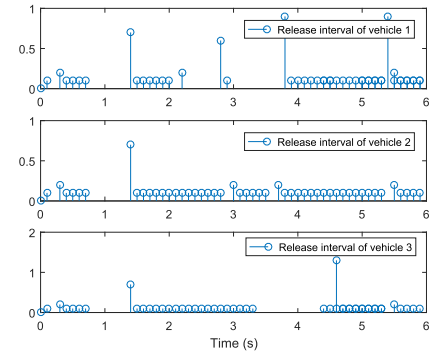


Fig. 9. Release instants and release intervals of vehicle 1–3 under Case 2.

TABLE III  
NUMBER OF RELEASED DATA PACKETS OF VEHICLE 1 WITHIN 6 s

	$h=0.01s$	$h=0.05s$	$h=0.1s$
TTM	600	120	60
ETM-CT	533	99	50
Learning-based ETM	529	79	32

TABLE IV  
NUMBER OF RELEASED DATA PACKETS OF VEHICLE 2 WITHIN 6 s

	$h=0.01s$	$h=0.05s$	$h=0.1s$
TTM	600	120	60
ETM-CT	519	94	44
Learning-based ETM	499	53	29

TABLE V  
NUMBER OF RELEASED DATA PACKETS OF VEHICLE 3 WITHIN 6 s

	$h=0.01s$	$h=0.05s$	$h=0.1s$
TTM	600	120	60
ETM-CT	535	101	51
Learning-based ETM	531	90	34

To further testify the superiority of the proposed learning-based ETM, a comparison is made among the TTM, the ETM with a constant threshold (ETM-CT) and our proposed learning-based ETM.

Tables III–V present the numbers of transmitted data packets of three vehicles with different sampling period  $h$  under the above three data-triggering mechanism.

By comparing the numbers of released data packets of three vehicles within 6s (as shown in Tables III–V), one can summarize that our proposed learning-based ETM can lead to a lower data requirement for secure path tracking of networked

AGVs with a certain level of control performance, which indicates that the implementation of learning-based ETM in this study can effectively economize the limited bandwidth.

## V. CONCLUSION

In this article, the problem of secure path tracking control of networked AGVs subject to deception attacks has been investigated by using a learning-based ETM. Each vehicle of AGVs is presumed as an agent, and the information interaction among vehicles is implemented via communication networks. To save network resources, the learning-based ETM, whose threshold is dependent on each vehicle state of AGVs, has been developed. In addition, the influences of deception attacks on the vehicle communication network are considered. Then, a new secure control strategy has been proposed for networked AGVs considering deception attacks. Through the use of Lyapunov stability theory and linear matrix inequality technique, sufficient conditions to ensure the stability of AGVs are obtained, and the controller gain is designed as well. Finally, the validity of the theoretical results is manifested through a simulated example. In the future, the attack detection and defense will be considered to improve the performance of networked AGVs subject to cyberattacks.

## APPENDIX A PROOF OF THEOREM 1

Consider the following Lyapunov-Krasovskii functional for system (18):

$$\begin{aligned} V(t) = & \delta^T(t)(I_{2N} \otimes P)\delta(t) + \int_{t-d_n}^t \delta^T(v)Q_1\delta(v)dv \\ & + \int_{t-d_m}^t \delta^T(v)Q_2\delta(v)dv + \int_{t-l_m}^t \delta^T(v)Q_3\delta(v)dv \\ & + d_n \int_{-d_n}^0 \int_{t+r}^t \dot{\delta}^T(v)R_1\dot{\delta}(v)dvdr \\ & + (d_m - d_n) \int_{-d_m}^{-d_n} \int_{t+r}^t \dot{\delta}^T(v)R_2\dot{\delta}(v)dvdr \\ & + l_m \int_{-l_m}^0 \int_{t+r}^t \dot{\delta}^T(v)R_3\dot{\delta}(v)dvdr. \end{aligned}$$

By calculating the derivation and mathematical expectation of  $V(t)$ , we can obtain that

$$\begin{aligned} \mathbf{E}\{\dot{V}(t)\} = & 2\delta^T(t)(I_{2N} \otimes P)\dot{\delta}(t) + \delta^T(t)(Q_1 + Q_2 + Q_3)\delta(t) \\ & - \delta^T(t - d_n)Q_1\delta(t - d_n) - \delta^T(t - d_m)Q_2\delta(t - d_m) \\ & - \delta^T(t - l_m)Q_3\delta(t - l_m) - l_m \int_{t-l_m}^t \dot{\delta}^T(v)R_3\dot{\delta}(v)dv \\ & - d_n \int_{t-d_n}^t \dot{\delta}^T(v)R_1\dot{\delta}(v)dv + \mathbf{E}\{\dot{\delta}^T(t)\mathfrak{R}\dot{\delta}(t)\} \\ & - (d_m - d_n) \int_{t-d_m}^t \dot{\delta}^T(v)R_2\dot{\delta}(v)dv \end{aligned} \quad (25)$$

where  $\mathbf{E}\{\dot{\delta}^T(t)\mathfrak{R}\dot{\delta}(t)\} = \mathbb{B}_1^T(t)\mathfrak{R}\mathbb{B}_1(t) + \rho^2\mathbb{B}_2^T(t)\mathfrak{R}\mathbb{B}_2(t)$ , wherein  $\mathfrak{R} = d_n^2R_1 + (d_m - d_n)^2R_2 + l_m^2R_3$ ,  $\mathbb{B}_1(t) = \bar{A}\delta(t) + \bar{E}F(x(t), t) + \rho B_1K_2\delta(t - d(t)) + \rho B_2K_1\epsilon(t) + \rho\bar{\beta}B_3K_2[\delta(t -$

$d(t)) + \delta(t - l(t))] - \rho\bar{\beta}B_4K_1\epsilon(t) + \rho\bar{\beta}B_4K_1\zeta(t - l(t))$ ,  $\mathbb{B}_2(t) = \rho B_3K_2[\delta(t - d(t)) + \delta(t - l(t))] + \rho B_4K_1\zeta(t - l(t)) - \rho B_4K_1\epsilon(t)$ .

From Assumption 2, it follows that

$$v^2\delta^T(t)H_2^T H_2\delta(t) - F^T(x(t), t)H_2^T H_2F(x(t), t) \geq 0. \quad (26)$$

According to (9) and (10), it has

$$\begin{aligned} -[(\mathcal{L}H_1\delta(t - d(t)))^T\sigma_a\Phi\epsilon(t) + \epsilon^T(t)\sigma_a\Phi\mathcal{L}H_1\delta(t - d(t))] \\ + \frac{2}{\mu}(\mathcal{L}H_1\delta(t - d(t)))^T\Phi\mathcal{L}H_1\delta(t - d(t)) \leq 0. \end{aligned} \quad (27)$$

It follows from (14) that

$$\theta^2[H_1\delta(t - l(t))]^T(I_N \otimes P)H_1\delta(t - l(t)) - \Gamma \geq 0 \quad (28)$$

where  $\Gamma = [\zeta^T(t - l(t)) - (I_N \otimes H)H_1\delta(t - l(t))]^T(I_N \otimes P)[\zeta^T(t - l(t)) - (I_N \otimes H)H_1\delta(t - l(t))]$ ,  $H_1 = [I_{2N} \ 0]$ ,  $H_2 = [0 \ I_{2N}]$ .

Combining (25)–(28), then applying the Jensen's inequality [27] and Schur complement yields that

$$\mathbf{E}\{\dot{V}(t)\} \leq \varpi^T(t)\Theta\varpi(t) \quad (29)$$

where  $\varpi(t) = [\delta^T(t) \ \delta^T(t - d_n) \ \delta^T(t - d(t)) \ \delta^T(t - d_m) \ \delta^T(t - l(t)) \ \delta^T(t - l_m) \ (H_2F(x(t), t))^T \ \epsilon^T(t) \ \zeta^T(t - l(t))]^T$ . Then, one can know that (20) and (21) are sufficient conditions to ensure  $\mathbf{E}\{\dot{V}(t)\} < 0$ , which implies that the networked AGVs are asymptotically stable in the mean-square sense. That completes the proof.

## REFERENCES

- [1] T. Weiskircher, Q. Wang, and B. Ayalew, "Predictive guidance and control framework for (semi-)autonomous vehicles in public traffic," *IEEE Trans. Control Syst. Technol.*, vol. 25, no. 6, pp. 2034–2046, Nov. 2017.
- [2] J. Ji, A. Khajepour, W. W. Melek, and Y. Huang, "Path planning and tracking for vehicle collision avoidance based on model predictive control with multiconstraints," *IEEE Trans. Veh. Technol.*, vol. 66, no. 2, pp. 952–964, Feb. 2017.
- [3] C. Hu, Z. Wang, Y. Qin, Y. Huang, J. Wang, and R. Wang, "Lane keeping control of autonomous vehicles with prescribed performance considering the rollover prevention and input saturation," *IEEE Trans. Intell. Transp. Syst.*, vol. 21, no. 7, pp. 3091–3103, Jul. 2020.
- [4] A. P. Aguiar and J. P. Hespanha, "Trajectory-tracking and path-following of underactuated autonomous vehicles with parametric modeling uncertainty," *IEEE Trans. Autom. Control*, vol. 52, no. 8, pp. 1362–1379, Aug. 2007.
- [5] R. Wang, H. Jing, C. Hu, F. Yan, and N. Chen, "Robust  $H_\infty$  path following control for autonomous ground vehicles with delay and data dropout," *IEEE Trans. Intell. Transp. Syst.*, vol. 17, no. 7, pp. 2042–2050, Jul. 2016.
- [6] C. Hu, R. Wang, F. Yan, and N. Chen, "Output constraint control on path following of four-wheel independently actuated autonomous ground vehicles," *IEEE Trans. Veh. Technol.*, vol. 65, no. 6, pp. 4033–4043, Jun. 2016.
- [7] R. Wang, C. Hu, F. Yan, and M. Chadli, "Composite nonlinear feedback control for path following of four-wheel independently actuated autonomous ground vehicles," *IEEE Trans. Intell. Transp. Syst.*, vol. 17, no. 7, pp. 2063–2074, Jul. 2016.
- [8] H. Yu, K. Meier, M. Argyle, and R. W. Beard, "Cooperative path planning for target tracking in urban environments using unmanned air and ground vehicles," *IEEE/ASME Trans. Mechatronics*, vol. 20, no. 2, pp. 541–552, Apr. 2015.
- [9] H. Bai, J. Shen, L. Wei, and Z. Feng, "Accelerated lane-changing trajectory planning of automated vehicles with vehicle-to-vehicle collaboration," *J. Adv. Transp.*, vol. 2017, pp. 1–11, Aug. 2017.
- [10] P. Stone and M. Veloso, "Multiagent systems: A survey from a machine learning perspective," *Auto. Robots*, vol. 8, no. 3, pp. 345–383, Jun. 2000.
- [11] L. Panait and S. Luke, "Cooperative multi-agent learning: The state of the art," *Auto. Agents Multi-Agent Syst.*, vol. 11, no. 3, pp. 387–434, Nov. 2005.

- [12] X. Hu, S. E. Li, and Y. Yang, "Advanced machine learning approach for lithium-ion battery state estimation in electric vehicles," *IEEE Trans. Transport. Electric.*, vol. 2, no. 2, pp. 140–149, Jun. 2016.
- [13] H. Reza Karimi and H. Gao, "New delay-dependent exponential  $H_\infty$  synchronization for uncertain neural networks with mixed time delays," *IEEE Trans. Syst., Man, Cybern. B, Cybern.*, vol. 40, no. 1, pp. 173–185, Feb. 2010.
- [14] H. Li, C. Wu, P. Shi, and Y. Gao, "Control of nonlinear networked systems with packet dropouts: Interval type-2 fuzzy model-based approach," *IEEE Trans. Cybern.*, vol. 45, no. 11, pp. 2378–2389, Nov. 2015.
- [15] W.-A. Zhang and L. Yu, "Output feedback stabilization of networked control systems with packet dropouts," *IEEE Trans. Autom. Control*, vol. 52, no. 9, pp. 1705–1710, Sep. 2007.
- [16] X. Yin, D. Yue, and S. Hu, "Adaptive periodic event-triggered consensus for multi-agent systems subject to input saturation," *Int. J. Control*, vol. 89, no. 4, pp. 653–667, Apr. 2016.
- [17] K. Lu, Z. Liu, C. L. P. Chen, and Y. Zhang, "Event-triggered neural control of nonlinear systems with rate-dependent hysteresis input based on a new filter," *IEEE Trans. Neural Netw. Learn. Syst.*, vol. 31, no. 4, pp. 1270–1284, Apr. 2020.
- [18] Z. Gu, C. K. Ahn, D. Yue, and X. Xie, "Event-triggered  $H_\infty$  filtering for T-S fuzzy-model-based nonlinear networked systems with multisensors against DoS attacks," *IEEE Trans. Cybern.*, early access, Nov. 5, 2020, doi: [10.1109/TCYB.2020.3030028](https://doi.org/10.1109/TCYB.2020.3030028).
- [19] L. Liu, Y.-J. Liu, A. Chen, S. Tong, and C. L. P. Chen, "Integral barrier Lyapunov function-based adaptive control for switched nonlinear systems," *Sci. China Inf. Sci.*, vol. 63, no. 3, Feb. 2020, Art. no. 132203.
- [20] L. Liu, Y.-J. Liu, D. Li, S. Tong, and Z. Wang, "Barrier Lyapunov function-based adaptive fuzzy FTC for switched systems and its applications to resistance-inductance-capacitance circuit system," *IEEE Trans. Cybern.*, vol. 50, no. 8, pp. 3491–3502, Aug. 2020.
- [21] Y. Shi, E. Tian, S. Shen, and X. Zhao, "Adaptive memory-event-triggered  $H_\infty$  control for network-based T-S fuzzy systems with asynchronous premise constraints," *IET Control Theory Appl.*, vol. 15, no. 4, pp. 534–544, Mar. 2021, doi: [10.1049/cth2.12059](https://doi.org/10.1049/cth2.12059).
- [22] A. Girard, "Dynamic triggering mechanisms for event-triggered control," *IEEE Trans. Autom. Control*, vol. 60, no. 7, pp. 1992–1997, Jul. 2015.
- [23] D. Yue, E. Tian, and Q.-L. Han, "A delay system method for designing event-triggered controllers of networked control systems," *IEEE Trans. Autom. Control*, vol. 58, no. 2, pp. 475–481, Feb. 2013.
- [24] X. Ge, Q.-L. Han, X.-M. Zhang, L. Ding, and F. Yang, "Distributed event-triggered estimation over sensor networks: A survey," *IEEE Trans. Cybern.*, vol. 50, no. 3, pp. 1306–1320, Mar. 2020.
- [25] Z. Gu, P. Shi, D. Yue, S. Yan, and X. Xie, "Memory-based continuous event-triggered control for networked T-S fuzzy systems against cyber-attacks," *IEEE Trans. Fuzzy Syst.*, early access, Jul. 29, 2020, doi: [10.1109/TFUZZ.2020.3012771](https://doi.org/10.1109/TFUZZ.2020.3012771).
- [26] E. Tian and C. Peng, "Memory-based event-triggering  $H_\infty$  load frequency control for power systems under deception attacks," *IEEE Trans. Cybern.*, vol. 50, no. 11, pp. 4610–4618, Nov. 2020.
- [27] Z. Gu, D. Yue, J. Liu, and Z. Ding, " $H_\infty$  tracking control of nonlinear networked systems with a novel adaptive event-triggered communication scheme," *J. Franklin Inst.*, vol. 354, no. 8, pp. 3540–3553, May 2017.
- [28] W. Li, Z. Xie, J. Zhao, and P. K. Wong, "Velocity-based robust fault tolerant automatic steering control of autonomous ground vehicles via adaptive event triggered network communication," *Mech. Syst. Signal Process.*, vol. 143, Sep. 2020, Art. no. 106798.
- [29] B. Shen, Z. Wang, D. Wang, and Q. Li, "State-saturated recursive filter design for stochastic time-varying nonlinear complex networks under deception attacks," *IEEE Trans. Neural Netw. Learn. Syst.*, vol. 31, no. 10, pp. 3788–3800, Oct. 2020.
- [30] S. J. Yoo, "Neural-network-based adaptive resilient dynamic surface control against unknown deception attacks of uncertain nonlinear time-delay cyberphysical systems," *IEEE Trans. Neural Netw. Learn. Syst.*, vol. 31, no. 10, pp. 4341–4353, Oct. 2020.
- [31] W. He, X. Gao, W. Zhong, and F. Qian, "Secure impulsive synchronization control of multi-agent systems under deception attacks," *Inf. Sci.*, vol. 459, pp. 354–368, Aug. 2018.
- [32] J. Liu, T. Yin, D. Yue, H. R. Karimi, and J. Cao, "Event-based secure leader-following consensus control for multiagent systems with multiple cyber attacks," *IEEE Trans. Cybern.*, vol. 51, no. 1, pp. 162–173, Jan. 2021.
- [33] Z. Gu, P. Shi, D. Yue, and Z. Ding, "Decentralized adaptive event-triggered  $H_\infty$  filtering for a class of networked nonlinear interconnected systems," *IEEE Trans. Cybern.*, vol. 49, no. 5, pp. 1570–1579, May 2019.
- [34] Y. Deng, X. Zhang, N. Im, G. Zhang, and Q. Zhang, "Model-based event-triggered tracking control of underactuated surface vessels with minimum learning parameters," *IEEE Trans. Neural Netw. Learn. Syst.*, vol. 31, no. 10, pp. 4001–4014, Oct. 2020.
- [35] Z. Luo, W. Xiong, J. Cao, and C. Huang, "Event-triggered state tracking for two-dimensional neural networks with impulsive learning control schemes," *J. Franklin Inst.*, vol. 357, no. 17, pp. 12364–12379, Nov. 2020.
- [36] X. Yang and H. He, "Decentralized event-triggered control for a class of nonlinear-interconnected systems using reinforcement learning," *IEEE Trans. Cybern.*, vol. 51, no. 2, pp. 635–648, Feb. 2021, doi: [10.1109/TCYB.2019.2946122](https://doi.org/10.1109/TCYB.2019.2946122).



**Zhou Gu** (Member, IEEE) received the B.S. degree from North China Electric Power University, Beijing, China, in 1997, and the M.S. and Ph.D. degrees in control science and engineering from the Nanjing University of Aeronautics and Astronautics, Nanjing, China, in 2007 and 2010, respectively.

From September 1996 to January 2013, he was with the School of Power Engineering, Nanjing Normal University, Nanjing, as an Associate Professor. He is currently a Professor with Nanjing Forestry University, Nanjing. His current research interests

include networked control systems, time-delay systems, reliable control, and their applications.



**Tingting Yin** received the B.S. degree in network engineering from the Nanjing University of Posts and Telecommunications, Yangzhou, China, in 2017, and the M.S. degree in software engineering from the Nanjing University of Finance and Economics, Nanjing, China, in 2020. She is currently pursuing the Ph.D. degree with the College of Mechanical and Electronic Engineering, Nanjing Forestry University, Nanjing.

Her research interests include T-S fuzzy systems, cyber-physical systems, and multi-agent systems.



**Zhengtao Ding** (Senior Member, IEEE) received the B.Eng. degree from Tsinghua University, Beijing, China, in 1984, and the M.Sc. degree in systems and control and the Ph.D. degree in control systems from the University of Manchester Institute of Science and Technology, Manchester, U.K., in 1986 and 1989, respectively.

He was a Lecturer with Ngee Ann Polytechnic, Singapore, for ten years. In 2003, he joined The University of Manchester, Manchester, where he is currently a Professor of control systems with the Department of Electrical and Electronic Engineering. He has authored the book "*Nonlinear and Adaptive Control Systems*" (IET, 2013) and a number of journal articles. His research interests include nonlinear and adaptive control theory and their applications.

Prof. Ding has served as an Associate Editor for the IEEE TRANSACTIONS ON AUTOMATIC CONTROL, *Transactions of the Institute of Measurement and Control*, *Control Theory and Technology*, *Mathematical Problems in Engineering*, *Unmanned Systems*, and the *International Journal of Automation and Computing*.